START

DRAFT
PREDECISIONAL
INFORMATION
5/12/88

APPENDIX G

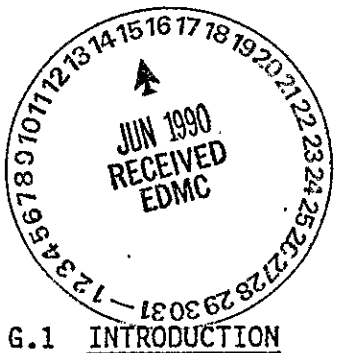

GROUNDWATER PATHWAY ASSESSMENTS

by
R. W. Nelson(a)
C. A. Oster(b)

G.1 INTRODUCTION

A series of groundwater pathway analyses for the 100-N accident scenarios were made using subsurface flow and transport models. The accident scenarios are described in Chapter 5 and Appendix D in detail so only the specifics involving the groundwater pathway flow and transport analysis are considered in detail in this appendix.

Two subsurface flow and transport modeling sequences were used in the analysis of the accident scenarios. The VTT model (Reisenauer 1979) and PATHS model (Nelson and Schur 1980) were both utilized. The VTT code was involved as a result of the previous modeling that had been done on the 1325-N Liquid Waste Disposal Facility (LWDF).(c) This VTT model was calibrated previously in a steady mode using 100-N subsurface data (Jensen 1987), but insufficient data were available for adequate transient calibration. The steady calibrated model, however, was used to provided the spatial hydraulic conductivity distribution for calculating an approximate equivalent homogeneous conductivity for use in the PATHS code. The PATHS model then was utilized to analyze the brief but extremely transient accident discharges to the 1325-N crib and trench.

(a) Staff Scientist, Hydrology Section, Battelle Pacific Northwest Laboratory.
(b) Systems Analyst/Programmer, Boeing Computer Services, Richland Inc.
(c) Nelson, R. W., N. J. Aimo, R. Schalla, and D. R. Newcomer. 1988. An Instrumented Vertical Plane for Evaluating Subsurface River Release Calculation Methods for the 1325 Liquid Waste Disposal Facility. WHC-IP-0315 PNL letter report to Westinghouse Hanford Co. 100-N Safety and Engineering Department dated January, 1988. 53pp.

In the sections to follow the groundwater model results from the earlier VTT calibration study are first presented. Next the basis is described for calculating the effective mean hydraulic conductivity to represent the spatially varying 100-N conductivity. This is followed by comparing the original VTT flow and arrival times with the steady PATHS results based on the calculated uniform hydraulic conductivity. The comparison will demonstrate that conservative river arrival results are provided by the PATHS model when using a geometric mean hydraulic conductivity. Next the water release sequence common to Accident scenarios #1, #2, #4 and #5, involving a 11-million gallon water release over 10.3 hours is routed (with seepage occurring), through the 1325-N crib and trench facility. This water release scenario effectively represents the maximum rate and duration of discharge to the LWDF that is possible without water over-flowing the facility and causing surface ponding with any associated overland flow. The seepage inflow sequence from the scenario water routing is next utilized in the PATHS model to determine the outflow rate of water and specific contaminant arrival distributions to the river. Use of the contaminant arrival distributions then allows the activity release rates to the river as a function of time to be provided for each particular nuclide or chemical contaminant released to the 1325-N crib and trench facility.

G.1.1 The 100-N Accident Release Scenarios to the LWDF Analyzed

There are four accident scenarios considered that release liquids directly to the 1325-N Liquid Waste Disposal Facility (LWDF) and one more major accident scenario where overflow from the lined-emergency basin [Liquid Effluent Retention Facility (LERF)] also reaches the LWDF. Therefore, five accident scenarios are considered here which result in potential releases to the Columbia River.

The details for all scenarios are described in Chapter 5, Section 5.2.2.2 and in Appendix D. Specifically, those considered hereafter are Accidents #1, #2, #4, and #5 which involve the maximum water release

sequence to the LWDF and Accident scenario #5C involving overflow from the LERF. The individual nuclide source term activities for these five scenarios are given in Tables G.1 through G.5.

G.2 PREVIOUS MODELING RESULTS USED

The results from previous modeling results of the 100-N Area and vicinity are a convenient starting place for the present evaluations. Though there had been earlier modeling (Nelson 1961, 1964; Cearlock 1970), the two more recent studies are most pertinent and provide the best starting point for this assessment (Nelson 1985, 1988).[(a)(b)] In the last of these two studies, a transient calibration of the two dimensional groundwater model of the 1325-N crib and trench ground disposal facility was undertaken; however, there were insufficient data to enable a satisfactory time dependent calibration of the VTT transient model. Accordingly, another approach than using the VTT model was required to handle the highly transient scenarios involved in the evaluations here.

The approach used was to build upon the available site information - including previous modeling results as much as possible and yet ensure the required transient analysis capacity was available. The flexible transient modeling capability of the PATHS code could be used for the large time variations in the accident scenarios if an equivalent homogeneous material were available. As much of the available previous information should still be used as is possible. Accordingly, the spatial hydraulic conductivity

---

(a) See Nelson, R. W., and A. E. Reisenauer. 1985. 1325-N Crib and Trench Groundwater Investigation. Letter Report prepared by PNL for Mr. Larry P. Diediker, Radioactive Control Group, United Nuclear Industries, November, 1985. 8pp.

(b) Nelson, R. W., N. J. Aimo, R. Schalla, and D. R. Newcomer. 1988. An Instrumented Vertical Plane for Evaluating Subsurface River Release Calculation Methods for the 1325 Liquid Waste Disposal Facility. WHC-IP-0315 PNL letter report to Westinghouse Hanford Co. 100-N Safety and Engineering Department dated January, 1988. 53pp.

TABLE G.1. Fission Product Inventory Discharged to the 1325-N LWDF for Accident #1 (Complete Blockage of Single Pressure Tube)

Nuclide[a]	Radioactive Half-Life	Total Inventory Discharged (Ci)	Act. Discharged Ao,(Ci/liter)[c]	Kd (ml/gm)	Retardation R
hydrogen-3	12 y	5.6×10^{0}	1.345×10^{-7}	0	1
chromium-51	27 d	1.2×10^{1}		20	97
iron-55	2.7 y	1.2×10^{2}	2.882×10^{-6}	50	242
iron-59	45 d	2.0×10^{1}		50	242
cobolt-60	5 y	4.9×10^{0}	1.177×10^{-7}	30	145
rubidium-86	19 d	8.0×10^{-2}		50	242
strontium-89	50 d	9.6×10^{2}	2.306×10^{-5}	10	49
strontium-90	29 y	9.2×10^{0}	2.210×10^{-7}	10	49
yttrium-90	29 y[b]	8.9×10^{0}		100	482
yttrium-91	59 d	1.1×10^{3}		100	482
zirconium-95	64 d	1.1×10^{3}		100	482
niobium-95	64 d[b]	5.8×10^{2}		50	242
technetium-99	213,000 y	1.7×10^{3}	4.083×10^{-5}	0	1
ruthenium-103	39 d	4.0×10^{3}		30	145
ruthenium-106	1 y	1.2×10^{2}	2.882×10^{-6}	30	145
tellurium-127	11 d[b]	4.4×10^{3}		5	25
tellurium-127m	11 d	2.7×10^{2}		5	25
tellurium-129	33 d[b]	2.2×10^{4}		5	25
tellurium-129m	33 d	4.0×10^{2}		5	25
iodine-131	8 d	4.9×10^{4}	1.177×10^{-3}	0	1
cesium-134	2 y	1.2×10^{1}		50	242
cesium-136	13 d	1.4×10^{2}		50	242
cesium-137	30 y	2.8×10^{2}	6.725×10^{-8}	50	242
barium-140	13 d	2.1×10^{3}		100	482
lanthanum-140	13 d[b]	2.1×10^{3}		100	482
cerium-141	35 d	1.5×10^{3}		100	482
cerium-144	284 d	2.8×10^{2}		100	482
praseodymium-143	13 d	1.9×10^{3}		100	482
neodymium-147	11 d	7.6×10^{2}		100	482
europium-154	8 y	2.8×10^{1}	6.723×10^{-7}	100	482
europium-155	5 y	2.9×10^{1}	6.963×10^{-7}	100	482
europium-156	15 d	3.3×10^{3}		100	482
plutonium	24,000 y	5.0×10^{-1}	1.201×10^{-8}	50	242

(a) Only the most significant radionuclides with half-lives greater than 8 days are listed in this table.
(b) These radionuclides are in equilibrium with longer-lived isotopes and effectively decay with the same half-life as the longer-lived isotope shown in this table.
(c) This column is the total inventory discharged (column 3) divided by the total water discharged in the scenario of $4.1635(10^{7})$ liters.

TABLE G.2. Fission Product Inventory Discharged to the 1325-N LWDF for Accident #2 (Double-Ended Break of Single Pressure Tube)

Nuclide[a]	Radioactive Half-Life	Total Inventory Discharged (Ci)	Act. Discharged Ao,(Ci/liter)	Kd (ml/gm)	Retardation R
chromium-51	27 d	1.0×10^{1}	2.402×10^{-7}	20	97
iron-55	2.7 y	1.0×10^{2}	2.402×10^{-6}	60	242
iron-59	46 d	1.7×10^{1}	4.083×10^{-7}	60	242
europium-154	8 y	2.4×10^{1}	5.764×10^{-7}	100	482
europium-155	5 y	2.4×10^{1}	5.764×10^{-7}	100	482
europium-156	15 d	2.7×10^{3}	6.485×10^{-5}	100	482

(a) Only the most significant radionuclides with half-lives greater than 8 days are listed in this table.

TABLE G.3. Fission Product Inventory Discharged to the 1325-N LWDF for Accident #4 (Reactor Trip with ECCS Demand, but Partial (1/16) Failure of ECCS)

Nuclide[a]	Radioactive Half-Life	Total Inventory Discharged (Ci)	Act. Discharged, Ao,(Ci/liter)[c]	Kd (ml/gm)	Retardation R
hydrogen-3	12 y	1.8×10^{2}	4.323×10^{-6}	0	1
rubidium-86	19 d	3.6×10^{0}		60	242
strontium-89	50 d	3.5×10^{4}	8.406×10^{-4}	10	49
strontium-90	29 d	3.2×10^{2}	7.686×10^{-6}	10	49
yttrium-90	29 y	3.2×10^{2}		100	482
yttrium-91	59 d	3.9×10^{4}		100	482
zirconium-95	64 d	4.0×10^{4}	9.607×10^{-4}	100	482
niobium-95	64 d	2.1×10^{4}		60	242
technetium-99	213,000 y	6.4×10^{4}	1.537×10^{-3}	0	1
ruthenium-103	39 d	1.4×10^{5}	3.363×10^{-3}	30	145
ruthenium-106	1 y	4.3×10^{3}	1.033×10^{-4}	30	145
tellurium-127	11 d[b]	1.6×10^{5}	3.843×10^{-3}	5	25
tellurium-127m	11 d	9.6×10^{3}		5	25
tellurium-129	33 d[b]	7.8×10^{5}	1.873×10^{-2}	5	25
tellurium-129m	33 d	1.6×10^{4}		5	25
iodine-131	8 d	1.8×10^{6}	4.323×10^{-2}	0	1
cesium-134	2 y	4.1×10^{2}	9.847×10^{-6}	60	242
cesium-136	13 d	5.8×10^{3}		60	242
cesium-137	30 y	1.0×10^{4}	2.402×10^{-4}	60	242
barium-140	13 d	7.5×10^{4}	1.801×10^{-3}	100	482
lanthanum-140	13 d	7.5×10^{4}		100	482
cerium-141	35 d	5.5×10^{4}		100	482
cerium-144	284 d	1.0×10^{4}	2.402×10^{-4}	100	482
praseodymium-143	13 d	6.9×10^{4}	1.657×10^{-3}	100	482
neodymium-147	11 d	2.7×10^{4}		100	482
plutonium	24,000 y	1.9×10^{1}	4.563×10^{-7}	60	242

(a) Only the most significant radionuclides with half-lives greater than 8 days are listed in this table.
(b) These radionuclides are in equilibrium with longer-lived isotopes and effectively decay with the same half-life as the longer-lived isotope shown in this table.
(c) This column is the total inventory discharged (column 3) divided by the total water discharged in the scenario of 4.1635 (10^{7}) liters.

TABLE G.4. Fission Product Inventory Discharged to the 1325-N LWDF for Accident #5 (Large LOCA with Complete Failure of ECCS, Loss of Confinement, and Unfiltered Stack Release)

Nuclide[a]	Radioactive Half-Life	Total Inventory Discharged (Ci)	Act. Discharged Ao,(Ci/liter)[c]	Kd (ml/gm)	Retardation R
hydrogen-3	12 y	2.8×10^{3}	6.725×10^{-5}	0	1
rubidium-86	19 d	2.60×10^{0}		50	242
strontium-89	50 d	2.4×10^{4}	5.764×10^{-4}	10	49
strontium-90	29 y	2.3×10^{2}	5.524×10^{-6}	10	49
yttrium-90	29 y[b]	2.2×10^{2}		100	482
yttrium-91	59 d	2.7×10^{4}		100	482
zirconium-96	64 d	2.8×10^{4}		100	482
niobium-95	64 d[b]	1.5×10^{4}		50	242
technetium-99	213,000 y	4.3×10^{4}	1.033×10^{-3}	0	1
ruthenium-103	39 d	1.0×10^{5}	2.402×10^{-3}	30	145
ruthenium-106	1 y	3.0×10^{3}	7.205×10^{-5}	30	145
tellurium-127	11 d[b]	1.1×10^{5}		5	25
tellurium-127m	11 d[b]	6.7×10^{3}		5	25
tellurium-129	33 d[b]	5.5×10^{5}	1.321×10^{-2}	5	25
tellurium-129m	33 d	1.2×10^{4}		5	25
iodine-131	8 d	1.8×10^{5}	4.323×10^{-2}	0	1
cesium-134	2 y	2.9×10^{2}	6.965×10^{-6}	50	242
cesium-136	13 d	3.5×10^{3}		50	242
cesium-137	30 y	7.0×10^{3}	1.681×10^{-4}	50	242
barium-140	13 d	5.2×10^{4}		100	482
lanthanum-140	13 d	5.2×10^{4}		100	482
cerium-141	35 d	3.8×10^{4}		100	482
cerium-144	284 d	7.1×10^{3}		100	482
praseodymium-143	13 d	4.8×10^{4}		100	482
neodymium-147	11 d	1.9×10^{4}		100	482
plutonium	24,000 y	1.3×10^{1}	3.122×10^{-7}	50	242

(a) Only the most significant radionuclides with half-lives greater than 8 days are listed in this table.
(b) These radionuclides are in equilibrium with longer-lived isotopes and effectively decay with the same half-life as the longer-lived isotope shown in this table.
(c) This column is the total inventory discharged of nuclides (column 3) divided by the total water discharged in the scenario of $4.1635(10^{7})$ liters.

TABLE G.5. Fission Product Inventory Discharged to the 1325-N LWDF for Accident #5C (Large LOCA with Complete Failure of ECCS, Confinement Success, and with LERF-SEP Upgrade)

Nuclide[a]	Radioactive Half-Life	Total Inventory Discharged (Ci)	Act. Discharged Ao, (Ci/liter)[c]	Kd (ml/gm)	Retardation R
hydrogen-3	12 y	1.4×10^{2}	6.166×10^{-5}	0	1
rubidium-86	19 d	1.0×10^{-1}		50	242
strontium-89	50 d	1.2×10^{3}	5.284×10^{-4}	10	49
strontium-90	29 y	1.1×10^{1}	4.844×10^{-6}	10	49
yttrium-90	29 y[b]	1.1×10^{1}		100	482
yttrium-91	59 d	1.4×10^{2}		100	482
zirconium-95	64 d	1.4×10^{3}		100	482
niobium-95	64 d	7.5×10^{2}		50	242
technetium	213,000 y	2.2×10^{3}	9.689×10^{-4}	0	1
ruthenium-103	39 d	5.0×10^{3}		30	145
ruthenium-106	1 y	1.5×10^{2}		30	145
tellurium-127	11 d	5.5×10^{3}		5	25
tellurium-127m	11 d	3.4×10^{2}		5	25
tellurium-129	33 d	2.8×10^{4}	1.233×10^{-2}	5	25
tellurium-129m	33 d	6.0×10^{2}		5	25
iodine-131	8 d	9.0×10^{4}	3.963×10^{-2}	0	1
cesium-134	2 y	1.5×10^{1}		50	242
cesium-136	13 d	1.8×10^{2}		50	242
cesium-137	30 y	3.5×10^{2}	1.541×10^{-4}	50	242
barium-140	13 d	2.6×10^{3}		100	482
lanthanum-140	13 d	2.6×10^{3}		100	482
cerium-141	35 d	1.9×10^{3}		100	482
cerium-144	284 d	3.6×10^{2}		100	482
praseodymium-143	13 d	2.4×10^{3}		100	482
neodymium-147	11 d	9.5×10^{2}		100	482
plutonium	24,000 y	8.7×10^{-1}	3.882×10^{-7}	50	242

(a) Only the most significant radionuclides with half-lives greater than 8 days are listed in this table.
(b) These radionuclides are in equilibrium with longer-lived isotopes and effectively decay with the same half-life as the longer-lived isotope shown in this table.
(c) This column is the total inventory discharged (column 3) divided by the total water discharged in the scenario of 2.271 (10^{9}) liters.

variations obtained from the earlier modeling calibrations were used to provide the best estimate for a representative uniform hydraulic conductivity.

G.2.1 Equivalent Uniform Hydraulic Conductivity

The spatial hydraulic conductivity distribution from the steady calibrated VTT model is shown in Figure G.1. The highest hydraulic conductivities of 120 m/day (393.7 ft/day) are seen midway along the 1325-N trench and diminishing values occurring elsewhere with lowest values of 40 to 50 m/day (131-164 ft/day) near the river.

The usual assumption that statistically the hydraulic conductivity is a logarithmic normal distribution leads to the traditionally accepted use of the geometric mean as the appropriate effective equivalent uniform conductivity (Gutjahr 1978; Neuman 1982). The geometric mean conductivity for the region in Figure G.1 between the dashed lines is 72 m/day (236.2 ft/day). The mean saturated thickness in this same region is 10.7 m (35.2 ft) above the underlying Ringold Clay, which is the effective bottom of the 1325-N subsurface flow system.

25 M/YEAR

G.2.2 Comparison of River Arrival Results

The results from the original steady calibrated VTT model will be compared to the PATHS model arrival times and cumulative outflows to the river. This will suggest the amount of conservatism that is involved in the more idealized PATHS analysis. Figure G.2 shows the groundwater flow and steady pathlines for a continuous discharge to the 1325-N facility of 3293 l/min (870 gal/min). The travel times along groundwater flow paths to the river range from a minimum time of 194 days to greater than a 1000 days.

The PATHS model was set up for the same steady case with a continuing inflow to the crib of 3293 l/min (870 gal/min), but with the equivalent uniform conductivity of 72 m/day and a saturated thickness of 10.7 m. Also in the PATHS code the 1325-N crib was represented as a circular inflow area rather than as a rectangle. A radius of 42.12 m (138.2 ft) was used, which

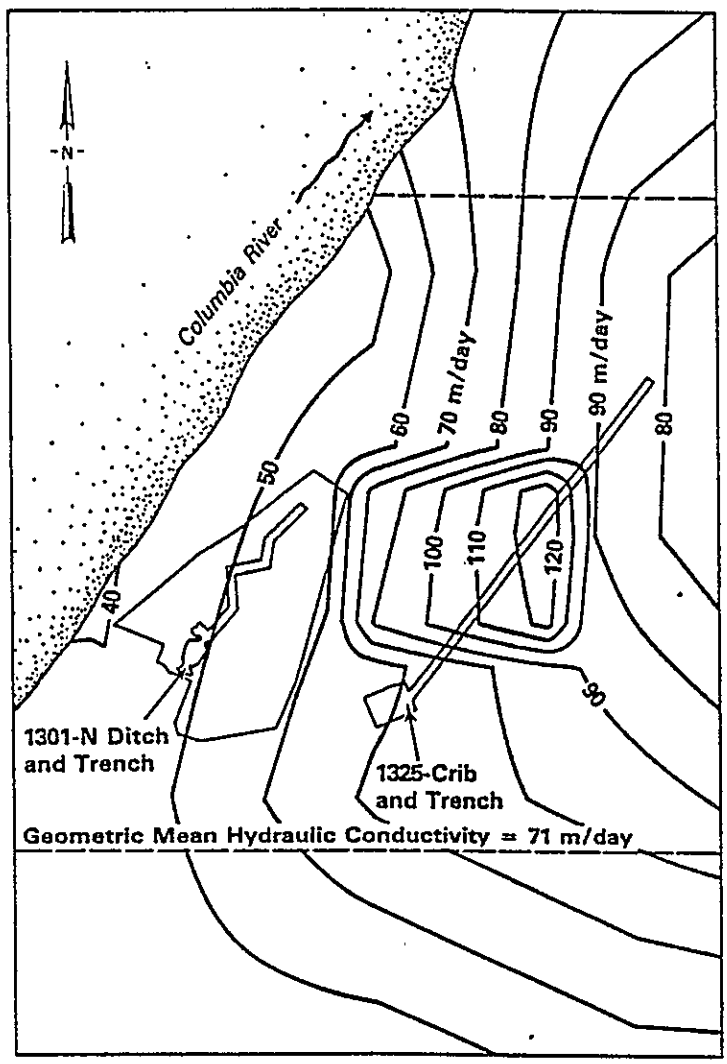

FIGURE G.1. Saturated Hydraulic Conductivity Distribution in the Vicinity of the 1325-N LWDF

is equivalent in area to the actual rectangular 73.2 x 76.2 m (i.e. 240 x 250 ft) crib. All of the other dimensions and hydrologic properties in the VTT and PATHS models were identical for the steady comparison.

The arrival results for the two models are tabulated in Table G.6. At the same cumulative fraction of the total flux, the arrival time of the PATHS model are always less than those from the VTT model. Accordingly the PATHS model results are in general conservative or tend to provide the worst case

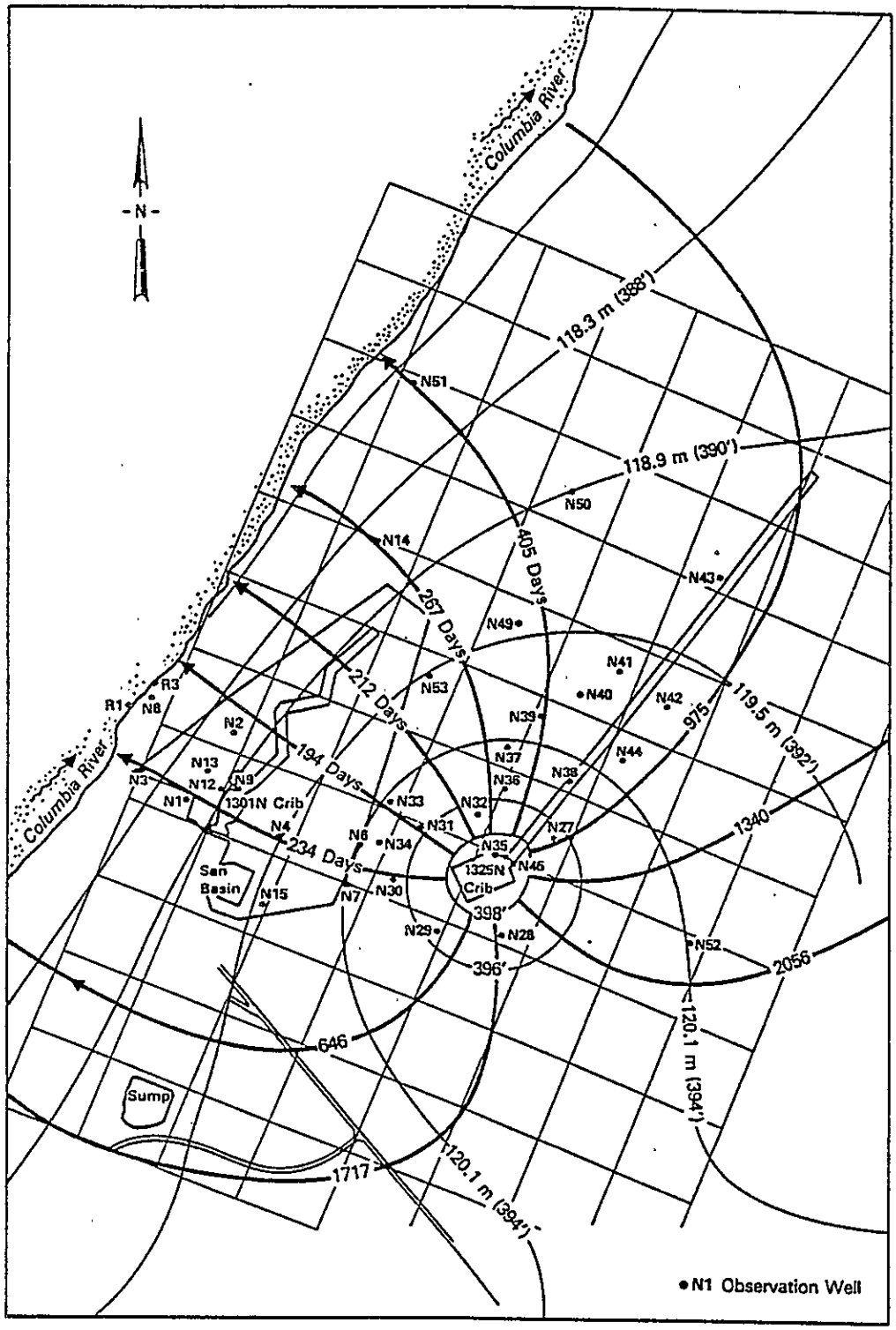

FIGURE G.2. Steady VTT Model Results for Continuous Disposal to the 1325-N Crib

TABLE G.6. Comparison of Contaminated Water Arrival Result of the VTT Model (Spatially Varying Material Properties) with the PATHS Model (Equivalent Homogeneous Material)

Cumulative Entering River, q/Qo	Arrival Time At River in Days After Discharge to 1325-N Crib	
	VTT model, days	PATHS model, days
0.00	193.58	184.09
0.05	197.24	186.22
0.10	202.71	189.48
0.15	211.85	197.66
0.20	222.80	206.41
0.25	241.07	220.83
0.30	262.98	237.21
0.35	299.51	255.08
0.40	350.64	286.15
0.50	509.52	360.07
0.60	774.33	469.84
0.70	1110.36	634.22
0.80	1519.44	892.33
0.90	2016.18	1363.94
0.90625	2534.84	2046.16
0.9875	---	2810.42

estimates for the two codes. This is seen more clearly in Figure G.3 where the arrival curves for the two sets of model results are plotted. The arrival curve for the PATHS model based on the equivalent homogeneous material is everywhere above and to the left of the variable VTT model curve. This shows that the PATHS analysis provides both higher outflow rates and shorter arrival times, which always results in higher predicted peak contaminant outflow rates and earlier contaminant arrival at the river (Nelson 1981). Accordingly, the more idealized model of the two yields results that are on the worst-case-estimate side of the analyses. Accordingly the PATHS

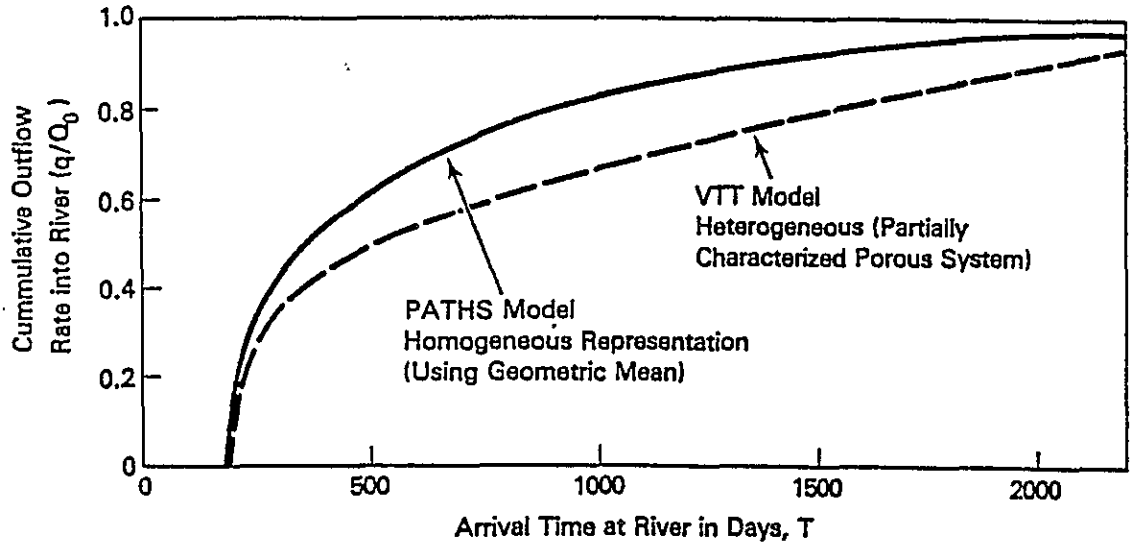

FIGURE G.3. Comparison of Contaminant Arrival Curves at River for Worst Case Homogeneous and Partially Characterized 100-N Subsurface System

model, which is capable of considering the very early and rapidly changing water releases in the 100-N accident scenarios, will be used as the primary tool for the groundwater pathway analysis.

G.3 ROUTING OF ACCIDENT SCENARIO WATER THROUGH THE LWDF

The water that is to be released in the accident scenarios must first be routed through the LWDF to determine when the water will first reach each particular part of the disposal facility. Such routing provides the starting time and duration of water infiltration from the crib and each of the four individual spillover sections in the 1325-N trench. The water routing procedure also provides any times of possible over-flow from the 1325-N crib and trench resulting from the discharge rate to the facility exceeding the combined infiltration and storage capacity of the crib and trench.

The release schedule in four of the accident scenarios (#1, #2, #4 and #5) involves 41.635 million liters (11 million gallons) of water discharged to the 1325-N LWDF at a rate of 67,373 l/min (17,800 gal/min). This gives a total time of water released to the facility of 10.3 hours. After this very

large accident release, the flow to the facility returns to the usual 3,141.55 l/min (830 gal/min) steady release rate of water to the crib and trench.

G.3.1 Effective Crib and Trench Infiltration Rates

The effective infiltration rate of water into the ground from the 1325-N crib has been studied in some detail. These studies were a result of the lower than expected intake rates that occurred during early use of the crib, which ultimately led to the construction of the trench. Pratt[(a)] reviewed the basis of the original design infiltration rate and provided the actual performance rates for the crib during the first 8 months of use. The as-built infiltration rate of 96 gal/day/sq ft by the end of the first 3 months had reduced to 36 gal/day/sq ft and continued diminishing during the next 3 months to 16 gal/day/sq ft. A month later the rate was 12 gal/day/ sq ft and the long-term steady rate was estimated to be 10 gal/day/sq ft. These rates were found to have occurred with an estimated water level in the crib of something less than 2 feet of head during the first 8 months of operation.

The short duration of the accident release scenarios combined with there being twice the usual head in the crib while the large discharge is occurring suggests that an effective infiltration rate of 20 to 25 gal/day/sq ft is a reasonable expected range. The use of the higher value in this range tends to lessen travel times so is the preferred worst case value. This higher rate is 1025 l/day/sq m or the total inflow rate into the ground from the entire crib area (73.2 m x 76.3 m) is 3,975 l/min. That flow rate into the ground reduces the total scenario discharge rate to 63,398 l/min (16,750 gal/min), which is actually the flow rate that is either contributing to temporary storage as the water level rises in the crib or spills over the discharge weir into the 1325-N trench.

(a) Pratt, D. R. 1984. "Appendix H: Permeability of the Glaciofluviatile Deposits at 100-N." Letter report prepared for UNC Nuclear Industries, Richland, Washington.

The rectangular discharge weir from the crib has a crest length of 1.83 m (6 ft) at a level 0.91 m (3 ft) above the bottom of the crib. There is a usable height above the weir crest to the crib ceiling of 0.61 m (2 ft). The discharge from the crib conforms nicely to the standard flow over a rectangular contracted weir, which is generally available in water control handbooks (see, for example, ARMCO 1949).

Water spilling over the crib weir enters the first of four cascading sections along the 914.4-m (3000-ft) length of the 1325-N trench. The trench bottom is level over the entire length, though the spill elevations for the three over-topping dams that form the cascading sections is each successively 0.3 m (1 ft) lower than the preceding dam spill level. Each of the over-topping dams, which are equally spaced at 228.6 m (750 ft) along the trench, has a small weir for measuring the overflow to the next cascading section during normal operations. These small weirs would be swamped and become completely ineffective control structures very soon after the large flow rates from the accident scenarios enter the trench.

Water infiltration from the rather long 1325-N trench is more conveniently expressed as the seepage rate per unit length of trench rather than per unit area as was used for the crib. Earlier studies of the expected infiltration from the trench are useful in providing the expected rates. Special prototype testing of a short length of the actual trench cross-section gave values ranging from 4240 gal/day/ft to 3139 gal/day/ft in the 4-day test.[a] In an analysis by Gee and Nelson[b], intake values ranged from a very conservative 1830 gal/day/ft to 5635 gal/day/ft. This latter highest figure was based upon the short-term test but used the minimum field measured hydraulic conductivity of 0.053 gal/min/sq ft at the prototype

---

(a) Pratt, D. R. 1984. "Appendix H: Permeability of the Glaciofluviatile Deposits at 100-N." Letter report prepared for UNC Nuclear Industries, Richland, Washington.

(b) Gee, G. W., and R. W. Nelson. 1985. Supporting Calculations and Recommendations for the Design of the Disposal Trench for 100-N Liquid Effluent (Project H-672). Letter report prepared by Pacific Northwest Laboratory for the Operations Division UNC Nuclear Industries, March 1985.

experimental trench site and the water level in the trench of 6.5 feet. Because the experimental site was in an area of likely equal or higher conductivity than occurs along the entire trench, a more appropriate conductivity is 0.044 gal/min/sq ft to be used with the higher scenario water level in the trench of 2.54 m (8.5 ft). For these conditions, the unit seepage rate from the trench is 36.43 l/min/m (4225 gal/day/ft) and the seepage rate from one cascading section of the trench becomes 8327 l/min (2200 gal/min).

G.3.2 Water Routing Through the 1325-N Crib

The water routing through the 1325-N crib involves balancing the inflow and outflow rates while accounting for interim storage during the water release scenario. It begins by reducing the total inflow rate to the crib by the steady infiltration rate into the ground. This net reduced inflow accumulates as storage in the crib until the water level rises to the crest of the outflow weir. The water level continues to rise with more and more water spilling over the weir with the increasing height. That increasing height of water above the weir crest also provides additional temporary storage in the crib. Such temporary storage continues increasing until the water level in the crib is high enough so the weir discharge rate just equals the effective inflow rate to the crib. Such a balance of inflow and outflow for the crib with a maximum of temporary storage will then continue until the scenario inflow rate to the crib ends.

The reverse of the process outlined for the water level build up in the crib starts to occur. With inflow to the crib reduced or shut off, the water level begins to gradually fall. As the level in the crib declines past the crest of the weir, further water discharge to the trench stops, but the water level gradually reduces still further as seepage from the crib into the ground continues.

The specific schedule and quantities obtained for the water routing through the 1325-N crib are summarized in Table G.7. As shown in the table, the first 80.3 minutes of the scenario is required to satisfy the infiltration into the ground and gradually fill the crib to the weir crest height of 0.91 m (3 ft). The volume stored in the crib as the water reaches the weir

TABLE G.7. Water Routing Summary Through 1325-N Crib

Time Since Scenario Began (minutes)	Effective Inflow Rate to Crib (liters/min)	Water Volume Stored in Crib (liters)	Discharge Rate Over Crib Weir (liters/min)	Comments
0.0	63,398	0.0	0.0	Accident started
80.3	63,398	5,096,128	0.0	Water Level
80.4	63,398	increasing	increasing	Reached Weir Crest
206.0	63,398	8,323,673	63,398	0.58 meter head
618.0	63,398	8,323,675	63,398	on weir (maximum
618.1	0.0	diminishing	decreasing	steady head)
745	0.0	5,096,128	0.0	Water Level Dropped to to Weir Crest
2027	0.0	0.0	0.0	Last Stored Water Seeped into Ground

crest is 5,096,128 liters. The next time period in the table (to reach 206 minutes) is required for the rising water level to reach equilibrium when the effective inflow rate to the crib is just equal to the weir discharge rate from the crib. This steady flow continues from 206 to 618 minutes (10.3 hrs) when the water inflow scenario to the crib ends. It then takes until time 745 for the water level in the crib to diminish to the weir crest elevation. It requires from time 745 to 2027 minutes later for all of the remaining stored water to seep into the ground from the crib.

G.3.3 Routing Through The 1325-N Cascading Trench

The water outflow over the wier from the crib is the beginning point for routing the flow through the four cascading sections of the 1325-N trench. Specifically from Table G.7, starting at 80.3 minutes, the first section of the trench begins receiving water. Initially this is at a moderate rate but increases significantly until at 206 minutes the rate entering the head of

the trench is 63,398 l/min. As previously stated, the spill-over weirs in the three cascading dams are so small that they are immediately swamped by the large flow rates down the trench, so any weir discharges are ignored. Accordingly all of the over-spill times and storage volumes in the routing are associated with the over topping of the rip-rapped dams separating the cascading sections of the trench.

The specific routing times, seepage rates, and total volumes entering the groundwater system are shown in Table G.8. From the first entry, seepage from the crib continues for the longest time due to the large combined static and dynamic storage capacity of the 1325-N crib. The four successive sections along the trench in the table each have longer time increments for the seepage into the ground. This results in slightly larger cumulative volumes entering groundwater as one progresses down the trench. The longer infiltration times result from the gradual diminishing flow rate down the trench caused from the continuing seepage into the ground as the water moves toward the end of the trench. For example, the second section of the trench fills slower than the first because of the intervening seepage which continues reducing the flow rate along the trench. This means that the last section of the trench takes the longest to fill because of the smaller flow rate. Once filled, however, the same time as for any of the other sections is required for that volume to enter the ground. But the total time available for seepage still remains longer by the extra filling time required.

All of the water seepage rates, times over which the contaminates enter the ground, and the total volumes entering the groundwater system for the four major release scenarios are provided in Table G.8. These are the specific scenario water inputs for use with the site characteristics in the PATHS code to evaluate the expected releases to the river.

G.4 PATHS MODEL EVALUATION OF THE FOUR ACCIDENT SCENARIOS

The PATHS model utilizes an analytical solution for the two dimensional flow system. Transient flow paths are provided using a modified fourth order

TABLE G.8. Water Routing Time Schedule, Seepage Rates and Total Volumes from the 1325-N Crib and Trench Entering the Groundwater System

Seepage Structure	Discharge Times to Structures Starting (min)	Ending (min)	Increment (min)	Rate of Seepage (liters/min)	Seepage Volume (liters)
1325-N Crib	0	2027.0	2027.0	3975	8,057,325
1st Section of Trench	80.4	1051.6	971.2	8327	8,087,182
2nd Section of Trench	207.9	1201.9	994.0	8327	8,277,038
3rd Section of Trench	358.2	1384.8	1026.6	8327	8,548,498
4th Section of Trench	541.1	1618.3	1077.2	8327	8,969,844
				Total	41,939,887

Runge-Kutta numerical integration scheme for solving the pair of two-dimensional pathline differential equations (Nelson and Schur 1978,1980).

G.4.1 Groundwater Analysis of Accident #1, #2, #4, and #5

The PATHS model was set up for the common discharge history of the four accident scenarios. In particular the flood routing results in the previous section provide the inflows and infiltration times. The model provided moderate flexibility and accuracy though the 1325-N trench had to be simulated using a line of wells. The analytical model did not have the capability to represent a trench so the line of wells was used as a good approximation. If enough closely spaced wells are used then the trench is represented very adequately. Accordingly, 24 wells spaced at 38.1 m (125 ft) were used to represent the trench. Each well receives steadily 1388 l/min for the discharge times shown in Table G.8 for the particular cascading sections of the trench in which the well was located.

The early rapid changing transient accident scenario required a very short integration time step during the initial 2 days of the PATHS model run. As the severity of the initial changes in time subsided then a longer time step could be used for the integration with considerably greater economy in the simulation runs. In this way the results were obtained with both good accuracy and solution economy. Some special effort was required to provide sufficient pathlines in the area of greatest interaction between the crib and

trench flow systems. The final result was a good distribution of arrival locations along the river with the associated arrival times. While generating these same pathlines the PATHS code also automatically set up the utility code runs necessary to calculate the groundwater outflow rates into the river as a function of the location along the river. In this way the complete results needed to evaluate the consequences of disposal to the crib and trench were obtained.

G.4.2 Contaminant Arrival Results for Accidents #1, #2, #4, and #5

The three interrelated factors required to evaluate the actual release to the river via groundwater from the accident discharges to the 1325 facility include:

- Where along the river does each pathline emerge?
- When does the contamination along each pathline arrive?
- How much water-transported contaminant emerges?

The required interrelationship of these three factors are provided from the PATHS modeling results. Specifically, the dependence of the first two are conveniently shown as curves of Outflow Locations versus Contaminant Arrival Times as in Figure G.4. The vertical ordinate is the outflow location along the river bank where the various flow paths emerge while the arrival times are shown as the horizontal ordinate expressed in days after the beginning of the accident discharge to the crib and trench. In the figure, the first and last arrival curves for the initially highly transient scenario discharge are shown. Because the release scenario is transient, the Outflow Location is the convenient linking variable between the above three variables. Accordingly, in Figure G.5 is shown the Outflow Location versus Contaminant Outflow Quantity curve. Only a single curve is seen in the figure even though this is a transient case; the early time variations gradually die out to give a steady flow as the contaminants proceed toward the river.

The contaminant arrival curves shown in Figures G.4 and G.5 are the complete groundwater flow and transport results for Accident #1, #2, #4, and

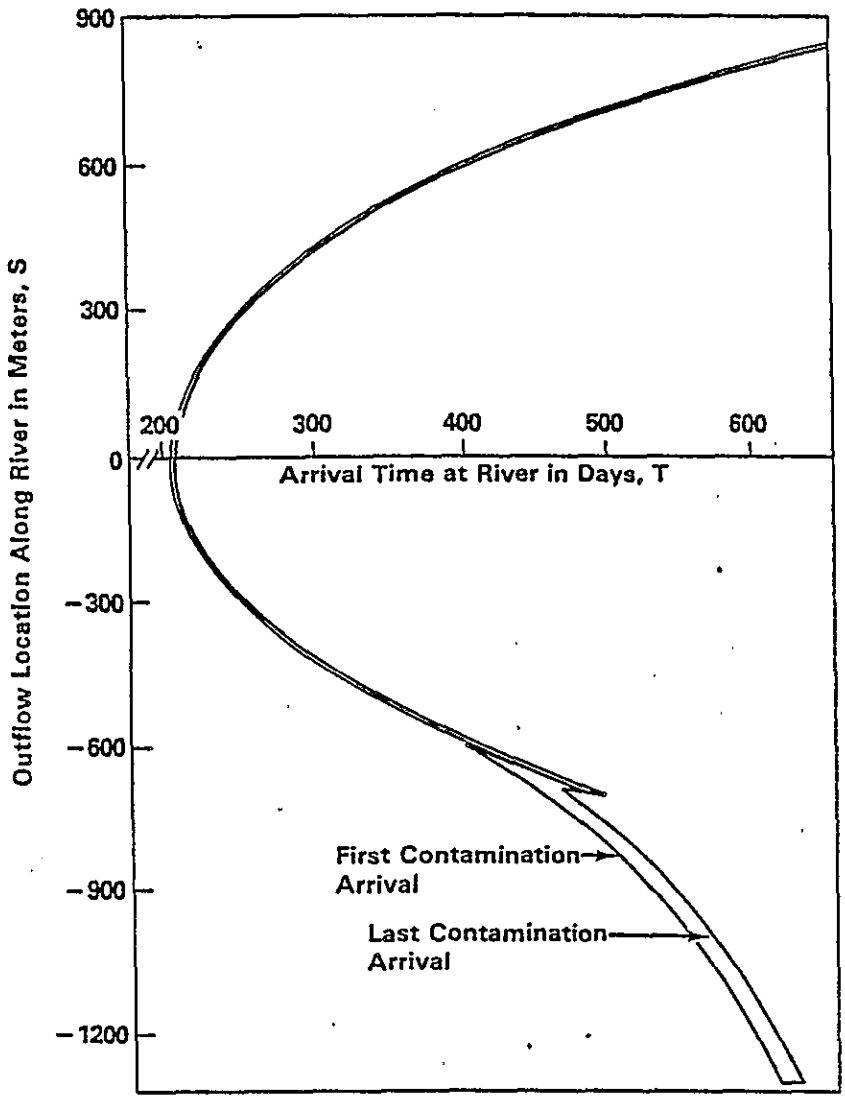

FIGURE G.4. Outflow Locations vs. Containment Arrival Times at the River for Accidents #1, #2, #4, and #5

#5 because the water releases to the crib and trench were the same. Additional groundwater flow and transport modeling for Accident #5C is required to provide the arrival curves at the river.

G.4.3 Analysis and Contaminant Arrival Results for Accident #5C

Accident #5C involves the release of a total of 2.271 million liters (600,000 gal) of water to the LWDF at a flow rate to the facility of

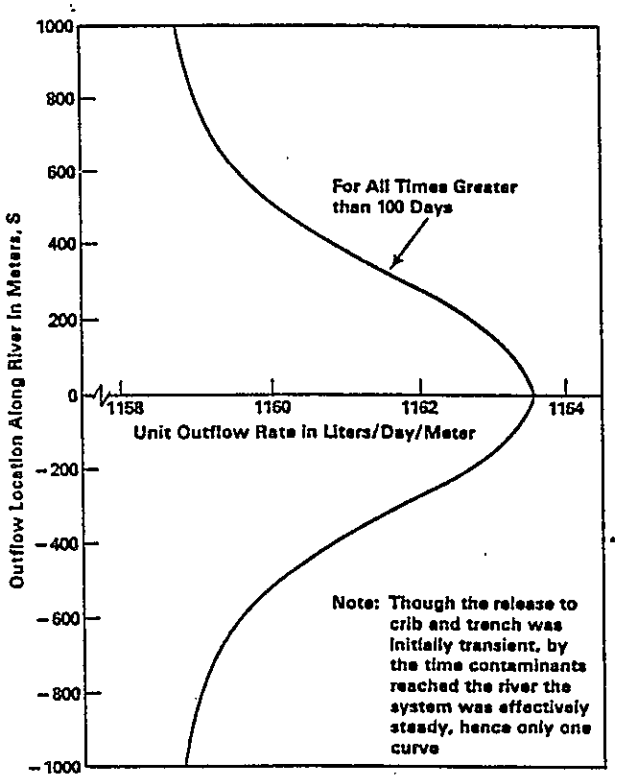

FIGURE G.5. Outflow Locations vs. Contaminated Water Outflow Rate per Unit Distance Along River for Accidents #1, #2, #4, and #5

67,393 l/min (17,800 gal/min). This means the discharge to the crib is for 33.7 min. With a seepage rate from the crib of 3,142 l/min (830 gal/min), less than half meter of the storage capacity of the crib is used. This means all of the Accident #5C water will enter groundwater by seepage from the crib. Water will never spill into the trench for this scenario. The total time for the contaminated water to seep into the ground from the crib is 0.5 day. Also, because the long term expected plant release to the LWDF is 3,142 l/min the PATHS model for Accident #5C is effectively a steady fluid flow system. The accident release simply replaces the usual operating plant discharge of water to the crib with the nuclide inventory involved in the scenario.

The contaminant arrival curves obtained from the PATHS model for Accident #5C are shown in Figures G.6 and G.7. Because the flow system is steady the

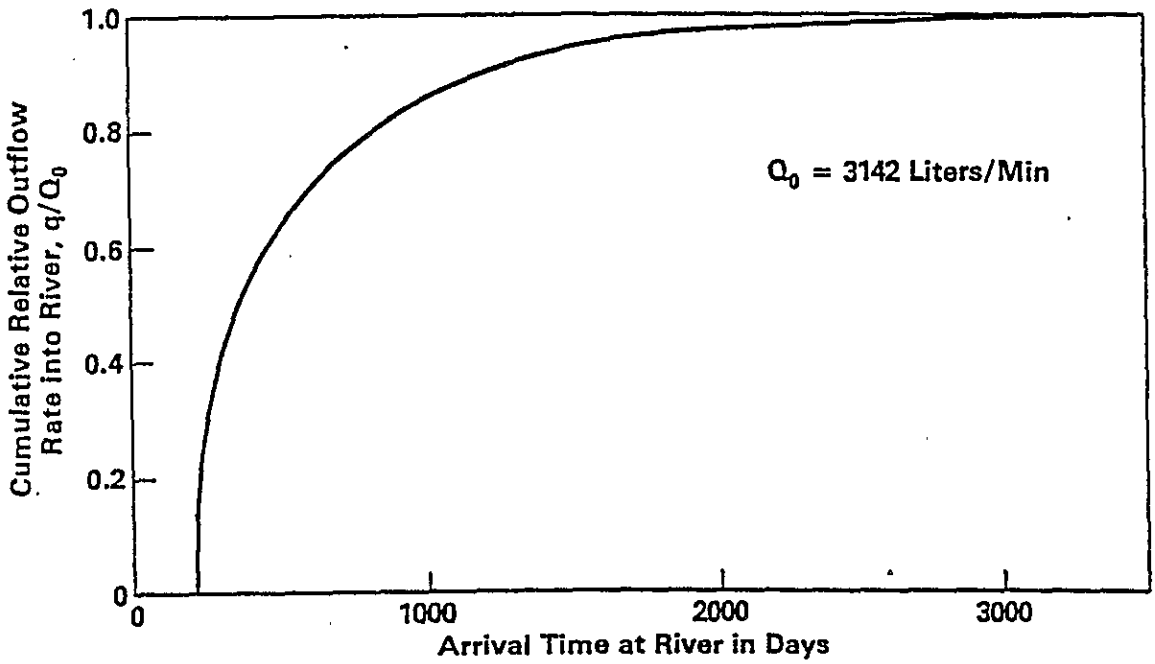

FIGURE G.6. Steady Cumulative Outflow Rate vs. Arrival Time at River for Accident #5C

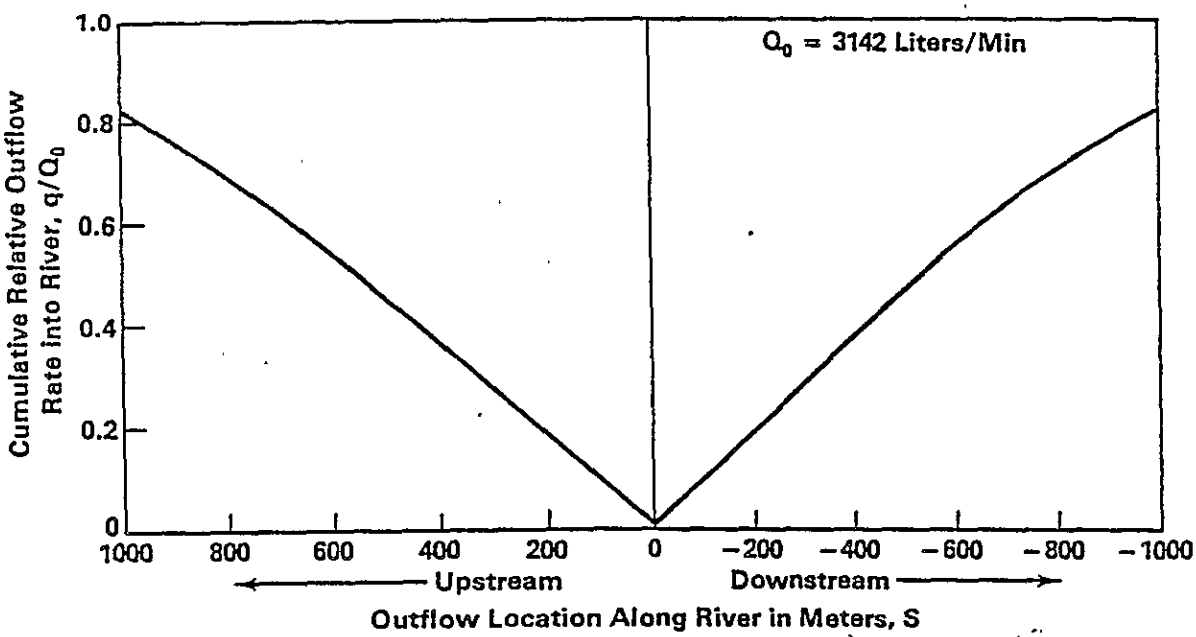

FIGURE G.7. Steady Cumulative Outflow Rate as a Function of Outflow Location Along the River for Accident #5C

more convenient cumulative relative outflow rate to the river is used as the linking variable for the two arrival curves (Nelson 1981). Before using the arrival results to provide the releases to the river, the retardation characteristics of the sediments in the 100-N groundwater system must be summarized.

G.4.4 The Kd Values for 100-N Soil for Various Radionuclides

There are numerous factors that enter into providing effective distribution sorption or K_d values for the variety of nuclides involved in the five accident scenarios. Also the difference in subsurface soils further complicate providing representative coefficients. With this in mind, the following assumptions were used to estimate K_d values for the radionuclides.

The first assumption is that the water released to the ground after a loss of coolant accident has a very low ionic strength with a neutral pH. This is based on the fact that the water originates as demineralized water or Columbia River water. There does not seem to be any data on the subsequent interactions with concrete, metal, or other reactor and containment building materials. As the volume of water is large and contact time prior to disposal to ground is short, it is assumed that little change in chemistry occurs. Thus K_d data for solutions that represent distilled water, river water, or potable ground waters were evaluated. (All accident scenarios are assigned the same K_d value.) If the waters react significantly with the reactor materials and dissolved large quantities of competing ions, the chosen K_d values will not be conservative. If the pH becomes acidic the K_d will not be conservative. If the pH becomes very basic (a possibility upon reaction with concrete) the K_d values of Cr, Fe, Co, Sn, La, Ce, Pr, Nd, Eu and Pu will likely be much higher.

The second assumption was that the Hanford sediments between the 1325-N crib and the river are rather coarse sedimentary quartz-rich sands with low cation-exchange capacities, minor carbonate contents, and low organic contents. This assumption is reasonable and effectively lowers K_d values (i.e. is conservative).

The third assumption is that the radionuclides are present in the cooling water as truly soluble species (not particulates) in their most common form (anion or cation) as designated on the table. The species ignore polymeric entities and when in doubt, the results of Baes and Mesmer (1976) were used. In reality, much of the radioactivity may be present as fine particulates, but the science of describing colloid transport is lacking, so it cannot be addressed.

The fourth assumption is that there is sufficient time for the cooling water and Hanford sediment to reach equilibrium before discharge into the river. If the travel times are at least a couple of weeks to a month, such an assumption is reasonable. If equilibrium is not reached, nuclide migration may exceed that predicted with accurate K_d values.

The fifth assumption is that the 1325-N crib has plenty of exchange capacity left even after normal usage. That is, the sorption sites are not already filled to a significant extent. If this assumption is incorrect, nuclide migration may exceed that predicted with accurate K_d values.

The sixth assumption is that the 1325-N hydrologic stream tubes do not intercept the old 1301-N contaminated sediments and desorb significant amounts of radionuclides disposed in the past. If significant desorption occurs, the nuclide migration may exceed that predicted.

The seventh assumption is that when there is a range of K_d data available it is best to use a low (conservative) value. This final assumption should help keep us from underestimating the migration rates if some of the other six assumptions are inaccurate.

Where no relevant data are available, best "technical judgement" was used. This involved considering data from United Nuclear Corporation (UNC) on the total curies discharged to cribs versus the amount emanating from the springs above the river (N-springs, Rokken 1987). These actual data give some relative estimates of mobility in 1985 and 1986. The effective K_d results are summarized in Table G.9.

TABLE G.9. The Soil K_d Values in ml/gm for 100-N Accident Scenarios

Nuclide	Species	Kd	Comment/Reference
^{3}H	H_2O	0	By convention ^{3}H to be HTO
^{51}Cr	$Cr(OH)^{2+}$	20	Nelson et al. 1966
$^{55,59}Fe$	$Fe(OH)^{2+}$	50	Estimate
^{60}Co	Co^{2+}	30	Conservative Hawkins 1964
^{86}Rb	Rb^{+}	50	Analogy to Cs
$^{89,90}Sr$	Sr^{2+}	10	Conservative McHenry 1958
$^{90,91}Y$	$Y(OH)^{2+}$	100	Analogy to lanthanides
^{95}Zr	$Zr(OH)_4°$	100	Conservative Rhodes 1957
^{95}Nb	$Nb(OH)_5°$	50	Estimate
$^{103,106}Ru$	Ru^{4+}	30	Conservative Rhodes 1957
$^{127,129}Te$	$TeO(OH)_3^-$	5	Estimate assuming selenite-selenate analog
^{131}I	I^-	0	Ames and McGarrah 1980
$^{134,136,137}Cs$	Cs+	50	Baetsle et al. 1964
^{140}Ba	Ba2+	100	Li and Chen 1979
^{140}La	La3+	100	Analogy to Ce
$^{141,144}Ce$	Ce3+	100	Rhodes 1957, Baethshe et al. 1962
^{143}Pr	Pr^{3+}	100	Analogy to Ce
^{147}Nd	Nd^{3+}	100	Analogy to Ce Rhodes 1957(a)
$^{154,155,156}Eu$	Eu^{3+}	100	Baetsle and Dejonghe 1962
Pu	PuO_2^+	50	Evans 1956, Rhodes 1957(b)

The soil K_d values in Table G.9 were used to calculate retardation factors, R using:

$$R = \frac{T_i}{T_w} = 1 + \frac{K_d B_d}{n} \quad (1)$$

where R = the retardation factor
T_i = the travel time of the individual ion
T_w = the travel time of the transporting water
B_d = the bulk density of the soil material (1.75 g/ml)
n = the porosity which may be ~~simulated as~~ calculated using:

~~Accordingly~~,

$$n = 1 - \frac{B_d}{P_d} = 1 - \frac{1.75}{2.75} = 0.364 \quad (2)$$

where P_d is the particle density of the material (2.75 g/ml)

and so from Equation (1)

$$R = 1 + 4.81\ K_d \quad (3)$$

which was the basis for calculating the last column in Tables G.1, G.2, and G.3, G.4 and G.5 for the various nuclides listed in those tables with the K_d values taken from Table G.9 above.

G.5 SUMMARY OF NUCLIDE RELEASES TO THE RIVER FROM SCENARIOS

The nuclide releases from each of the scenarios were used with the corresponding groundwater arrival curves at the river of the previous sections to obtain the specific nuclide releases to the river. The auxiliary support computer code FLXACT was used to combine the groundwater arrival results with the specific nuclide inventory taking into account decay and any retardation resulting from soil sorption interactions if such occur. These particular nuclide sources and the retardation when occurring for specific nuclides from Tables G.1 through G.5 are combined with the groundwater transport arrival

distributions in the FLXACT analysis. The results provided by the support code are the activity and the outflow rate of each nuclide entering the river as a function of time.

The outflow curve for tritium from Accident #5 into the Columbia River is shown in Figure G.8. This is the highest tritium result in all the analyses and two results are shown. The irregular curve is the total instantaneous outflow rate of tritium in curies per day as a function of time. It represents the total tritium inflow integrated at every location along the river bank where tritium is entering the river. Also shown in the same figure as the smooth declining curve is the maximum activity in curies per liter (see right-hand scale) entering the river with time. If a time is selected from the figure, for example 612 days where the peak inflow rate occurs with an associated activity of $6.1(10^{-5})$ Ci/liter, more information is available. Use of the 612 days in Figure G.4 indicates specifically where the tritium is entering the river at that time. From the latter figure the inflow-activity

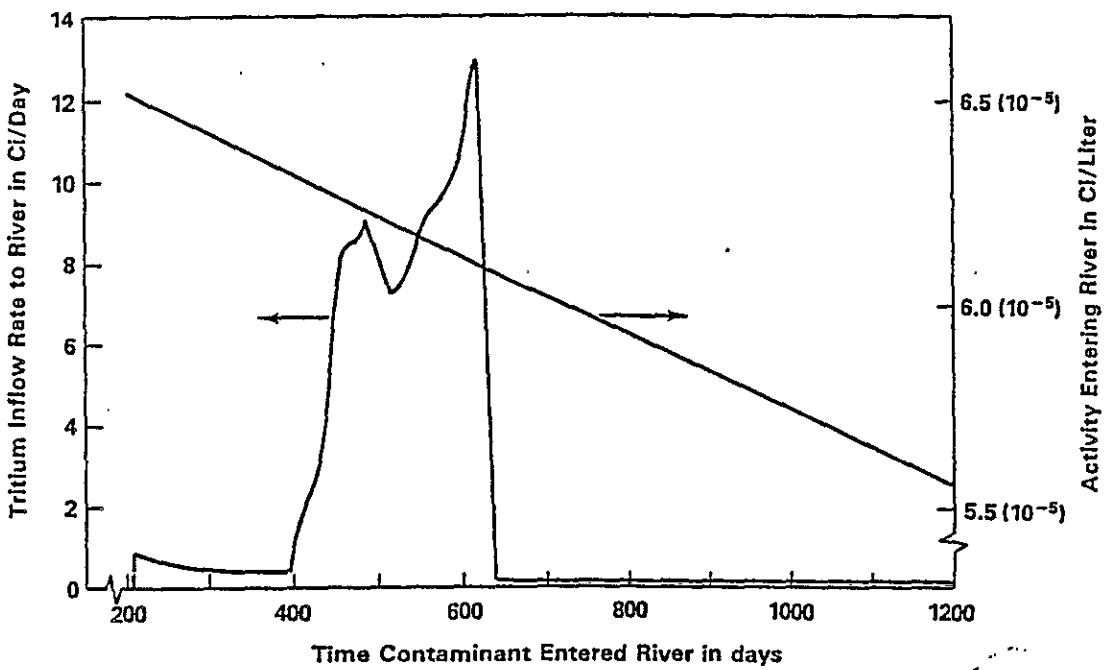

FIGURE G.8. Tritium Activity and Flow Rate into River with Time for Accident Scenario #5

of 6.1(10^{-5}) Ci/liter enters the river downstream between -1165 meters and -1280 meters as well as upstream between 824 and 842 meters.

Another outflow curve for tritium to the river from Accident #5C is shown in Figure G.9. This curve is somewhat more typical of the contaminant outflow curves for nuclides in the scenarios because there is only one peak at the early-on arrival. When such a single peak occurs it always appears at very near the first containment arrival.

The specific inventories entering for each of the five accident scenarios analyzed are given in Tables G.10, G.11, G.12, G.13, and G.14 respectively for scenarios #1, #2, #4, #5 and #5C. In these summary tables, three times when containments reach the river are provided, namely first contaminent arrival, last contaminant arrival, and the arrival time of the peak outflow rate entering the river. Also the activity in Ci/liter at the time of peak activity outflow rate is provided along with the integrated total inventory

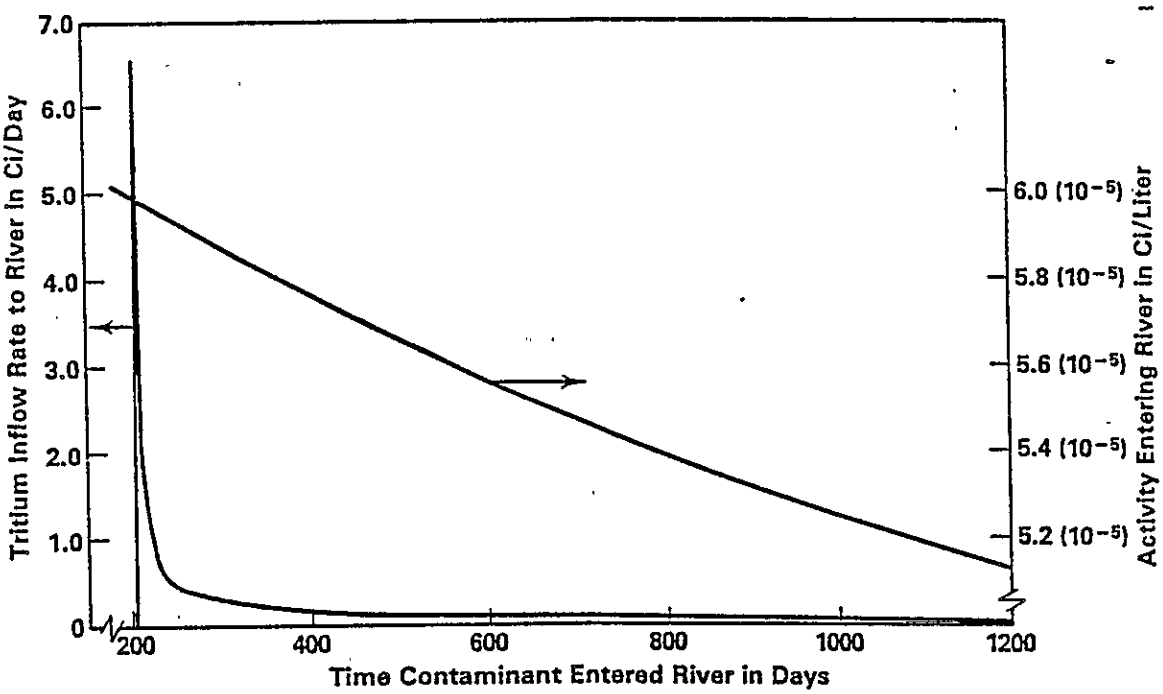

FIGURE G.9. Tritium Outflow Rate and Activity Entering the River with Time for Accident Scenario #5C

TABLE G.10. Fission Product Inventory Discharged to the 1325-N LWDF and Entering the River via Groundwater for Accident #1 (Complete Blockage of Single Pressure Tube)

Nuclide	Total Inventory Discharged (Ci)	Times Contaminant Enters River: First Arrival (Days)	Last Arrival (Days)	Peak (Days)	Peak Activity (Ci/l)	Peak Activity Outflow (Ci/day)	Total Inventory Entering River (Ci)
hydrogen-3	5.6×10^{8}	206	2,445	612	1.22×10^{-7}	2.59×10^{-2}	4.15×10^{8}
chromium-51	1.2×10^{1}						
iron-55	1.2×10^{2}	---	---	---	0.00	0.00	0.00
iron-59	2.8×10^{1}						
cobalt-60	4.9×10^{8}	29,986	122,856	29,963	1.35×10^{-12}	1.14×10^{-10}	4.28×10^{-7}
ribidium-86	8.8×10^{-2}						
strontium-89	9.6×10^{2}	---	---	---	0.00	0.00	0.00
strontium-90	9.2×10^{8}	10,124	119,994	22,897	5.205×10^{-8}	1.402×10^{-4}	1.338×10^{8}
yttrium-90	8.9×10^{8}						
yttrium-91	1.1×10^{3}						
zirconium-95	1.1×10^{3}						
niobium-95	5.8×10^{2}						
technetium-99	1.7×10^{3}	206	2445	612	4.882×10^{-5}	8.878×10^{8}	1.384×10^{3}
ruthenium-103	4.8×10^{3}						
ruthenium-106	1.2×10^{2}	---	---	---	0.00	0.00	0.00
tellurium-127	4.4×10^{3}						
tellurium-127m	2.7×10^{2}						
tellurium-129	2.2×10^{4}						
tellurium-129m	4.6×10^{2}						
iodine-131	4.9×10^{4}	206	512	208	1.758×10^{-11}	2.158×10^{-7}	5.217×10^{-6}
cesium-134	1.2×10^{1}						
cesium-136	1.4×10^{2}						
cesium-137	2.8×10^{2}	49,797	596,187	49,799	2.882×10^{-7}	1.464×10^{-5}	2.538×10^{-1}
barium-140	2.1×10^{3}						
lanthanum-140	2.1×10^{3}						
cerium-141	1.5×10^{3}						
cerium-144	2.8×10^{2}						
praseodymium-143	1.9×10^{3}						
neodymium-147	7.6×10^{2}						
europium-154	2.8×10^{1}	99,388	198,611	99,396	3.87×10^{-17}	9.84×10^{-16}	1.69×10^{-11}
europium-155	2.9×10^{1}	---	---	---	0.00	0.00	8.66×10^{-18}
europium-156	3.3×10^{3}						
plutonium	5.8×10^{-1}	49,797	596,187	147,317	1.187×10^{-8}	1.844×10^{-5}	4.826×10^{-1}

TABLE G.11. Fission Product Inventory discharged to the 1325-N LWDF and Entering the River via Groundwater for Accident #2 (Double-Ended Break of Single Pressure Tube)

Nuclide	Total Inventory Discharged (Ci)	Times Contaminant Enters River: First Arrival (Days)	Last Arrival (Days)	Peak (Days)	Peak Activity (Ci/l)	Peak Activity Outflow (Ci/day)	Total Inventory Entering River (Ci)
chromium-51	1.0×10^{1}	---	---	---	0.00	0.00	0.00
iron-55	1.0×10^{2}	---	---	---	0.00	0.00	4.24×10^{-16}
iron-59	1.7×10^{1}						
europium-154	2.4×10^{1}	99,388	202,422	99,398	3.32×10^{-17}	8.44×10^{-16}	9.34×10^{-12}
europium-155	2.4×10^{1}	---	---	---	0.00	0.00	6.67×10^{-18}
europium-156	2.7×10^{3}						

TABLE G.12. Fission Product Inventory Discharged to the 1325-N LWDF and Entering the River via Groundwater for Accident #4 (Reactor Trip with ECCS Demand, but Partial (1/16) Failure of ECCS)

Nuclide	Total Inventory Discharged (Ci)	Times Contaminant Enters River: First Arrival (Days)	Last Arrival (Days)	Peak (Days)	Peak Activity (Ci/l)	Peak Activity Outflow (Ci/day)	Total Inventory Entering River (Ci)
hydrogen-3	1.8×10^{2}	206	2445	612	3.924×10^{-6}	8.333×10^{-1}	1.33×10^{2}
rubidium-86	3.0×10^{0}						
strontium-89	3.5×10^{4}	---	---	---	0.00	0.00	0.00
strontium-90	3.2×10^{2}	16,124	119,993	22,997	1.810×10^{-8}	4.877×10^{-3}	4.654×10^{1}
yttrium-90	3.2×10^{2}						
yttrium-91	3.9×10^{4}						
zirconium-95	4.0×10^{4}	---	---	---	0.00	0.00	0.00
niobium-95	2.1×10^{4}						
technetium-99	6.4×10^{4}	206	2445	612	1.537×10^{-3}	3.264×10^{2}	5.211×10^{4}
ruthenium-103	1.4×10^{5}	---	---	---	0.00	0.00	0.00
ruthenium-106	4.3×10^{3}	---	---	---	0.00	0.00	0.00
tellurium-127	1.6×10^{5}	---	---	---	0.00	0.00	0.00
tellurium-127m	9.6×10^{3}						
tellurium-129	7.8×10^{5}	---	---	---	0.00	0.00	0.00
tellurium-129m	1.6×10^{4}						
iodine-131	1.8×10^{6}	206	502	208	6.46×10^{-10}	7.89×10^{-8}	1.916×10^{-4}
cesium-134	4.1×10^{2}	---	---	---	0.00	0.00	0.00
cesium-136	5.0×10^{3}						
cesium-137	1.0×10^{4}	49,797	598,186	49,806	1.029×10^{-5}	5.23×10^{-4}	9.66×10^{0}
barium-140	7.5×10^{4}	---	---	---	0.00	0.00	0.00
lanthanum-140	7.5×10^{4}						
cerium-141	5.5×10^{4}						
cerium-144	1.0×10^{4}	---	---	---	0.00	0.00	0.00
praseodymium-143	6.9×10^{4}	---	---	---	0.00	0.00	0.00
neodymium-147	2.7×10^{4}						
plutonium	1.9×10^{1}	49,797	598,187	147,317	4.51×10^{-7}	3.97×10^{-4}	1.529×10^{1}

TABLE G.13. Fission Product Inventory Discharged to the 1325-N LWDF and Entering the River via Groundwater for Accident #5 (Large LOCA with Complete Failure of ECCS, Loss of Confinement, and Unfiltered Stack Release)

Nuclide	Total Inventory Discharged (Ci)	Times Contaminant Enters River: First Arrival (Days)	Last Arrival (Days)	Peak (Days)	Peak Activity (Ci/l)	Peak Activity Outflow (Ci/day)	Total Inventory Entering River (Ci)
hydrogen-3	2.8×10^{3}	206	2,445	612	6.186×10^{-5}	1.297×10^{1}	2.87×10^{3}
rubidium-86	2.8×10^{0}						
strontium-89	2.4×10^{4}	---	---	---	0.00	0.00	0.00
strontium-90	2.3×10^{2}	10,124	119,993	22,097	1.361×10^{-6}	3.504×10^{-3}	3.344×10^{1}
yttrium-90	2.2×10^{2}						
yttrium-91	2.7×10^{4}						
zirconium-95	2.8×10^{4}						
niobium-95	1.5×10^{4}						
technetium-99	4.3×10^{4}	206	2445	612	1.033×10^{-3}	2.194×10^{2}	3.502×10^{4}
ruthenium-103	1.0×10^{5}	---	---	---	0.00	0.00	0.00
ruthenium-106	3.0×10^{3}	---	---	---	0.00	0.00	0.00
tellurium-127	1.1×10^{5}						
tellurium-127m	6.7×10^{3}						
tellurium-129	5.5×10^{5}	---	---	---	0.00	0.00	0.00
tellurium-129m	1.2×10^{4}						
iodine-131	1.8×10^{6}	206	532	298	6.455×10^{-10}	7.895×10^{-6}	1.918×10^{-4}
cesium-134	2.9×10^{2}	---	---	---	0.00	0.00	0.00
cesium-136	3.5×10^{3}						
cesium-137	7.8×10^{3}	49,797	598,186	49,800	7.203×10^{-6}	3.660×10^{-4}	6.374×10^{0}
barium-140	5.2×10^{4}						
lanthanum-140	5.2×10^{4}						
cerium-141	3.8×10^{4}						
cerium-144	7.1×10^{3}						
praseodymium-143	4.8×10^{4}						
neodymium-147	1.9×10^{4}						
plutonium	1.3×10^{1}	49,797	598,186	147,317	3.886×10^{-7}	2.715×10^{-4}	1.947×10^{1}

TABLE G.14. Fission Product Inventory Discharged to the 1325-N LWDF and Entering the River via Groundwater for Accident #5C (Large LOCA with Complete Failure of ECCS, Confinement Success, and with LERF SEP Upgrade)

Nuclide	Total Inventory Discharged (Ci)	Times Contaminant Enters River: First Arrival (Days)	Last Arrival (Days)	Peak (Days)	Peak Activity (Ci/l)	Peak Activity Outflow (Ci/day)	Total Inventory Entering River (Ci)
hydrogen-3	1.4×10^{2}	206	3324	287	5.967×10^{-5}	6.567×10^{0}	9.870×10^{1}
rubidium-86	1.8×10^{-1}						
strontium-89	1.2×10^{3}	---	---	---	0.00	0.00	0.00
strontium-90	1.1×10^{1}	10,121	183,161	10,122	2.498×10^{-6}	5.669×10^{-3}	2.265×10^{0}
yttrium-90	1.1×10^{1}						
yttrium-91	1.4×10^{2}						
zirconium-95	1.4×10^{3}						
niobium-95	7.5×10^{2}						
technetium-99	2.2×10^{3}	206	3324	208	9.689×10^{-4}	3.521×10^{1}	1.685×10^{3}
ruthenium-103	5.0×10^{3}						
ruthenium-106	1.5×10^{2}						
tellurium-127	5.5×10^{3}						
tellurium-127m	3.4×10^{2}						
tellurium-129	2.0×10^{4}	---	---	---	0.00	0.00	0.00
tellurium-129m	6.0×10^{2}						
iodine-131	9.0×10^{4}	206	3324	287	6.648×10^{-10}	7.317×10^{-5}	9.348×10^{-5}
cesium-134	1.5×10^{1}						
cesium-136	1.8×10^{2}						
cesium-137	3.5×10^{2}	49,788	495,341	49,781	6.610×10^{-6}	3.953×10^{-3}	2.622×10^{0}
barium-140	2.6×10^{3}						
lanthanum-140	2.6×10^{3}						
cerium-141	1.9×10^{3}						
cerium-144	3.6×10^{2}						
praseodymium-143	2.4×10^{3}						
neodymium-147	9.5×10^{3}						
plutonium	7.0×10^{-1}	49,788	882,512	49,781	3.979×10^{-7}	1.418×10^{-4}	5.256×10^{-1}

that enters the river. In the summaries for each scenario in general, a single peak occurred as is illustrated in Figure G.9 when the first and peak arrival times are very close together. When the peaks occur at some latter time between the first and last arrival times, then multiple peaks of the type shown in Figure G.8 occurred. When zeros appear in the tables, the activity, activity flow rates, and total inventory entering the river involved were less than 10^{-20} curies. Also in cases where no entries occur in the tables, it was readily apparent that insignificant releases to the river would occur. When no results are shown in Tables G.10 through G.13, the results were totally insignificant. The reader may usually verify that fact simply by referring to other tables in the sequence for that same nuclide where results will be found for a higher release concentration to the ground of that isotope.

G.6 REFERENCES

ARMCO. 1949. Handbook of Water Control. Calco Division ARMCO Drainage and Metal Products, Inc., Berkeley, California.

Ames, L. L., and J. E. McGarrah. 1980. Basalt-Radionuclide Distribution Coefficient Determinations, FY 1979 Annual Report. PNL-3146, Pacific Northwest Laboratory, Richland, Washington.

Baetsle, L., and P. Dejonghe. 1962. "Investigations on the Movement of Radioactive Substances in the Ground. Part III. Practical Aspects of the Program and Physicochemical Considerations." In Ground Disposal of Radioactive Wastes, TID-7628, pp. 198-210.

Baetsle, L. H., P. Dejonghe, W. Maes, W. E. Simpson, J. Souffriau, and P. Staner. 1964. Underground Radionuclide Movement, EURAEC-703.

Cearlock, D. B. and R. D. Mudd. 1970. Analysis of Hydrologic Factors Influencing the Operation of the 100-N Emergency Waste Disposal Crib. BNWL-1503, Pacific Northwest Laboratory, Richland, Washington.

Evans, E. J. 1956. Plutonium Retention in Chalk River Soil. CRHP-660, Chalk River, Ontario, Canada.

Gutjahr, A. L., et al. 1978. Stochastic Analysis of Spatial Variability in Subsurface Flows, Part II, Evaluation and Application: Water Resource Research. V. 14, no. 5, p. 953-960.

Hawkins, D. B. 1964. Removal of Cobalt and Chromium by Precipitation and Ion Exchange on Soil, Lignite, and Slinoptilolite from Citrate-Containing Radioactive Liquid Waste. IDO-12036, Idaho Falls, Idaho.

Jensen, E. J. 1987. Summary of Water Level Measurements Around the 1325N Crib During the Fall of 1985 and the Winter of 1986-87. PNL-6374, Pacific Northwest Laboratory, Richland, Washington.

Li, Y. -H, and L. -H Chan. 1979. "Desorption of Ba and ^{226}Ra from River-Borne Sediments in the Hudson Estuary." Earth Planet Sci. Letters 43:343-350.

McHenry, J. R. 1958. "Ion Exchange Properties of Strontium in a Calcareous Soil." Soil Science Society of America, Proceedings 22:514-518.

Nelson, J. L., R. W. Perkins, J. M. Neilsen, and W. L. Hauschild. 1966. Reactions of Radionuclides from the Hanford Reactors with Columbia River Sediments. IAEA-SM-72/8, pp. 139-161. International Atomic Energy Agency, Vienna, Austria.